Living in future ocean acidification, adaptive responses of sea urchins resident at a CO_2 vent system

Oriana Migliaccio[1], Annalisa Pinsino[2], Elisa Maffioli[3], , Abigail M. Smith[4], Claudio Agnisola[5], Valeria Matranga[2], Simona Nonnis[3], Gabriella Tedeschi[3], Maria Byrne[4], Maria Cristina Gambi[6], Anna Palumbo[1]

[1]Stazione Zoologica Anton Dohrn, Department of Biology and Evolution of Marine Organisms, Naples, Italy

[2]Istituto di Biomedicina e Immunologia Molecolare "Alberto Monroy", Consiglio Nazionale delle Ricerche, Palermo, Italy

DIMEVET. – Section of Biochemistry, University of Milan, Milan, Italy

[4]Schools of Medical and Biological Science, University of Sydney, Sydney, Australia

[5]Department of Biology, University of Naples Federico II, Napoli, Italy

[6]Stazione Zoologica Anton Dohrn, Department of Integrative Marine Ecology (Villa Dohrn-Benthic Ecology Center), Ischia, Naples, Italy

Correspondence

Anna Palumbo

Department of Biology and Evolution of Marine Organisms

Stazione Zoologica Anton Dohrn,

Villa Comunale, 80121 Naples, Italy

Email: anna.palumbo@szn.it

Key words: Ocean acidification, sea urchins, adaptation, Eco-physiology, proteomics

Running head: sea urchin response to acidification

Primary Research Article

Formattato: Non Evidenziato

Formattato: Non Evidenziato

Codice campo modificato

ABSTRACT

Ocean acidification (OA) is one of the most pervasive anthropogenic impacts on marine life. OA effects have been mainly investigated in laboratory/mesocosm experiments. However, to what extent these *in vitro* studies can be extrapolated to the natural environment is questionable. We used the Castello CO_2 vents at Ischia, Naples, Italy, as a natural laboratory to study the long-term effects of OA on the sea urchin *Paracentrotus lividus* population resident in low-pH, pH~7.8, focusing on the immune system. Seven months of animal tracking at the vent site confirmed their long-term site fidelity. Comparison of *P. lividus* from the vent and two control sites was used to assess putative adaptation to low-pH in coelomic fluid pH, immune cells number, phenotype, proteome and intracellular redox state, animal metabolism and skeletal mineralogy. There were no changes in the pH of the coelomic fluid, number and percentage of immune cells type in vent animals. Immune cell proteomics showed that 311 proteins were differentially expressed in urchins across sites with a general shift towards antioxidant processes in the vent urchins. Total antioxidant capacity was higher in immune cells from the vent urchins, while lipid-hydroperoxides and nitric oxide levels were not different. Moreover, the levels of phagosome and microsomal proteins were higher in the vent immune cells, suggesting an increased defence activity. These urchins also show an up-regulation of several enzymes of ammonium metabolism, amino-acid degradation, and modulation of many proteins of carbon metabolism. No changes in respiration, nitrogen excretion and skeletal mineralogy were observed. Our results reveal the mechanisms adopted by immune cells in the sea urchin adaptation to low pH/high pCO_2 and suggest that the long-term exposure to OA conditions, commensurate with near-future global change projections, does not negatively influence the health of *P. lividus* at the vent.

INTRODUCTION

Ocean uptake of anthropogenic CO_2 is decreasing surface ocean pH (ocean acidification – OA) and the saturation state (Ω) of the carbonate ions (CO_3^{2-}) required by a large diversity of marine species to make their shells and skeletons (Albright et al., 2016; Gattuso et al., 2015; IPCC, 2014). Ocean acidification, as a global stressor, is altering the function of marine ecosystems, with particular impacts on calcifying organisms, such as sea urchins, oysters, crabs, and corals (Barry et al., 2014; Doney et al., 2012; Kroeker, Micheli, & Gambi, 2013a). Our understanding of the effects of OA has mainly been limited to laboratory studies (eg. Kroeker, Kordas, Crim, & Singh, 2010; Przeslawski, Byrne, & Mellin, 2015) where decreases in calcification rates, enhancement of metal toxicity, variations in organism physiological indices (survival, growth, development, metabolism), modification in the gene and/or protein expression are reported (Byrne, Lamare, Winter, Dworjanyn, & Uthicke, 2013; Carey, Harianto, & Byrne, 2016; Lewis et al., 2016).

Natural CO_2 vent systems have greatly enhanced our understanding of the impacts of OA on populations and the consequences at the community and ecosystem levels (Connell, Kroeker, Fabricius, Kline, & Russell, 2013; Foo, Byrne, Ricevuto, & Gambi, 2018). These acidified sites incorporate a range of environmental factors, such as nutrients, currents and species interactions, not easily replicated in the laboratory (Barry, Hall-Spencer, & Tyrrell, 2010; Garrard et al., 2012). Although CO_2 vents are open systems and so mobile fauna may not spend their entire life in the vents, these systems are particularly useful in providing insights into future ocean conditions, especially in investigations of species that have resided these areas for years to decades. Indeed, many of the findings of investigations undertaken at vent systems have reinforced many of the trends observed in laboratory studies (Foo et al., 2018).

One of the best characterised CO_2 vent systems that have been investigated in a global change context are the shallow water systems around the Castello Aragonese in Ischia Island in the Mediterranean Sea (Hall-Spencer et al., 2008; Foo et al., 2018). In this location, shallow rocky reef habitat and sea grass beds occur in low-pH conditions, providing an important opportunity to investigate responses of associated biodiversity to OA and assess implications for ecosystem function. Importantly, the gas emissions at the Ischia site are primarily carbon dioxide (90–95%) and are not associated with any known toxic compounds or increased temperature conditions (Hall-Spencer et al., 2008; Tedesco, 1996; Italiano, Pecoraino, Gambi, unpublished data). In this regard the Ischia vents differ from other sites (e.g. Vulcano Island, Sicily, White Island, New Zealand) where CO_2 gas release is associated with toxic trace elements, sulphides and/or thermal increase (Tarasov, 2006; Vizzini et al., 2013).

Paracentrotus lividus is a key species in Mediterranean benthic communities, where it controls the dynamic, structure and composition of shallow macroalgal assemblages through its grazing activity (Boudouresque & Verlaque, 2013; Bulleri, Benedetti-Cecchi, & Cinelli, 1999; Sala et al., 1998). Sea urchins are facing the impact of increasing anthropogenic pressures in coastal environments, including eutrophication, warming, hypoxia, pollution, harmful algal blooms and OA (Bögner, 2016; Burnell, Russell, Irving, & Connell, 2013; Castellano et al., 2016; Matranga, Toia, Bonaventura, Müller, 2000; Migliaccio et al., 2016; Morroni, Pinsino, Pellegrini, Regoli, & Matranga, 2016; Pinsino et al., 2008). *Paracentrotus lividus* is an important food source for fishes and other animals (Guidetti & Mori, 2005), including humans that consider its gonads a culinary delicacy. The condition of *P. lividus* and its safety as food are therefore of great interest at multiple levels.

At the Ischia vents there have been several studies of the resident sea urchins *P. lividus* and *Arbacia lixula*, because, as calcifiers, they are expected to be negatively affected by increased organism pCO_2 (Byrne et al., 2013; Hall-Spencer et al., 2008; Kroeker et al., 2013a; Kroeker, Gambi, & Micheli, 2013b; Nogueira et al., 2017). In particular, *P. lividus* does not occur at the extreme low-pH zones (pH 6.6, pH 7.2), but the populations that reside at the pH 7.8 zone do not show any difference in abundance and size compared to those living in adjacent control pH 8.1 areas (Hall-Spencer et al., 2008; Kroeker et al., 2013a, 2013b), although their foraging area is lower than that recorded for urchins at the control zones (Kroeker et al., 2013b). In the Vulcano vent system *P. lividus* appears less resilient to acidification than *A. lixula* (Calosi et al., 2013a).

Here we assessed the health status of the population of *P. lividus* resident at the Ischia CO_2 vent systems in comparison with that for populations from ambient conditions using a number of metabolic and stress markers, focusing on the coelomic and immune systems. Sea urchin health status is typically assessed through determination of their physiological conditions, immune cell behaviour and coelomic fluid profile (Pinsino et al., 2015). The coelomic fluid functions similar to the blood of higher animals in which the immune cells reside (Bodnar, 2013; Pinsino et al., 2015). Sea urchin immune cells comprise a heterogeneous population of freely moving cells in the coelomic fluid and body tissues. These cells are considered the sentinels of environmental stress in sea urchins (Pinsino & Matranga, 2015). Sea urchins exhibit a considerable capacity to adapt/adjust to environmental changes and perturbations due to their responsive immune system in the expansion and diversification of immune genes, a response that provides protection, robustness, and molecular plasticity (Pinsino & Matranga, 2015). Investigation of the biochemistry of the coelomic fluid of *P. lividus* and other sea urchin species exposed to low pH in short (days-weeks) (Collard et al., 2013; Lewis

et al., 2016) and longer (months) (Dworjanyn & Byrne, 2018; Uthicke, Liddy, Nguyen, & Byrne, 2014) term exposures show that they can regulate their coelomic pH, at least at pH 7.7-7.8. In addition, *P. lividus* amd *A. lixula* translocated to vent sites for 2-4 days exhibited no change in the pH of their coelomic fluid but had a higher pCO_2, an observation taken to suggest the ability to regulate acid–base status in high pCO_2 (Calosi et al., 2013a). Sea urchins achieve their acid-base homeostasis through uptake of bicarbonate and this is suggested to incur a high energetic cost (Collard et al., 2013; Dubois, 2014). The increase in the metabolic rate of sea urchins held for two months in OA also indicates higher metabolic costs at low pH (Carey et al., 2016), although the respiratory response of urchin acclimated to OA conditions is highly variable, with no clear trends (Catarino, Bauwens, & Dubois, 2012; Kurihara, Yin, Nishihara, Soyano, & Ishimatsu, 2013; Stumpp, Trübenbach, Brennecke, Hu, & Melzner, 2012; Uthicke, Soars, Foo, & Byrne, 2013).

Recent studies have investigated the effect of exposure to low pH on sea urchin immune cells. *Heliocidaris erythrogramma* held under OA conditions exhibited a change in the profile of the immune cells within days, but with adjustment to background levels over time - weeks (Brothers, Harianto, McClintock, & Byrne, 2016). Lipid peroxidation in immune cells of *P. lividus* does not change after short exposure to OA (Lewis et al., 2016). With respect to the skeleton, the mechanical properties of the test of *P. lividus* maintained in OA conditions in the laboratory for 1 year and those resident at the Vulcano vents did not differ from *P. lividus* living in control conditions (Collard et al., 2016).

While laboratory studies indicate the physiological buffer capability of sea urchins in response to decreased pH on relatively short timescales, our understanding of the effects of OA on populations naturally living in low-pH conditions is poor, especially in term of

proteins and mechanisms involved in immune tolerance. In this study, we focused on the immune cells of *P. lividus* living at the natural CO_2 vents along Castello Aragonese in Ischia Island (pH~7.8) integrating a "high-throughput" approach into ecology by comparative analysis with immune cells from two control sites with normal ambient pH conditions (pH~8.12). We also investigated whole organism physiological responses with respect to acid-base balance (coelomic fluid pH), respiration, nitrogen metabolism and skeletal mineralogy to compare the responses of *P. lividus* resident at the vent and control sites. The latter trait has been shown to differ in *P. lividus* translocated to vent sites (Calosi et al., 2013a). As this species is relatively sedentary and has a limited home range, it is likely that the study animals were resident at the vent sites for most of their life and their physiology and biochemistry reflect acclimatisation to the life at low pH. To confirm that the urchins were resident, we monitored individuals *in situ* for seven months. Comparative analysis of immune cell activity-based protein profiling in sea urchins collected from low pH and control zones was examined through shotgun and label free proteomic technology. The number, phenotypes and intracellular redox status of the immune cells was also characterized.

Overall, our analyses provided insights as to how sea urchins can thrive in low pH/high pCO_2 conditions. The wide range of parameters examined allowed an understanding of the molecular mechanisms responsible for the hypothesized acclimatisation of *P. lividus* living at the vent site. Our findings indicate that long-term acclimatisation to the vent environment does not negatively affect the health status of *P. lividus* and that this is associated with an enhancement in immune cells antioxidant capability and defence activity, and modulation of several enzymes involved in metabolic pathways.

MATERIALS AND METHODS

Collection sites

Paracentrotus lividus (test diameter: 5.03 ± 0.51, 4.97 ± 0.60 and 4.9 ± 0.55 cm for C1, C2 and N2, respectively; n = 10 per site; all individuals with the gonadosomatic index GSI >1) were collected from three sites, one venting area and two non-venting control sites. The venting area site (mean pH is 7.8 ± 0.2; Kroeker, Micheli, Gambi, & Martz, 2011; Ricevuto, Kroeker, Ferrigno, Micheli F, & Gambi, 2014) is located in shallow water (~0.5 to 3m depth) in the north side (N2) of Castello Aragonese. Ischia Island (40°44'48.3"N, 13°56'39.6"E) (Tyrrhenian Sea, Italy) (Fig. S1). Control site one (C1) was located at S. Pietro Point, Ischia Island (40°44'48.3"N, 13°56'39.6"E) approximately 4 km west from the Castello vent area. This site (pH 8.1; Calosi et al., 2013b; Kroeker et al., 2011) was chosen because, except for pH, the other parameters, such as exposure of the rocky reef habitat, light, hydrodynamic conditions, temperature, salinity and depth, are very similar to the vent habitat (Calosi et al., 2013b). The second control site (C2) was near Naples, at Castel dell'Ovo (40°49'40.9"N, 14°14'49.5"E) approximately 40 km east of the vent area (Migliaccio et al., 2016).

At the time of sea urchin collection, also seawater samples from each site were collected for determination of salinity, temperature, pH, partial pressure of CO_2, total alkalinity, bicarbonate, carbonate concentrations, and the saturation states for calcite and aragonite. The data for the vent site were similar to those reported from long term monitoring (since 2007, see Ricevuto et al., 2014). The water temperature of each site was logged with *in situ* Hobo sensors throughout the duration of the observation periods (approx. 1 year).

The sea urchins were transported in cool boxes with water from the habitat (5 L/animal) and transported to the Anton Dohrn laboratory within an hour of collection. They were placed in closed recirculating tanks, connected to external aquarium filters unit (Pratiko Askoll) and filled with natural seawater (salinity 38 PSU). Temperature was maintained at 18 ± 2°C with

12:12 light: dark cycle and daily measured. Seawater pH in each aquarium was monitored with a pH meter (HI98150, HANNA), calibrated with standard NIST buffers. In the tank with the animals collected in the acidified N2 station, the pH was maintained at pH_{NIST} 7.7-7.8, with a CO_2 bubbling and a pH controller system: "CO2 energy professional" system (Ferplast) comprising digital pH controllers (mod. AQUA2001) connected to pH electrodes. Animals were maintained in these conditions for maximum 48 hours before the analysis. No spawning or mortality occurred during this period.

Monitoring the sea urchins from the low pH site using non-invasive tagging

P. lividus specimens at the N2 zone were monitored by using a non-invasive tagging technique, allowing the identification of each animal and its permanence at the site. On August 2014, the location of sea urchins (~ 4 cm diameter) was marked by placing numbered steel spikes and stakes adjacent to their burrows/location on rock reef and in the *Posidonia oceanica* meadows, respectively. Identification was assisted by recording the color and the diameter (cm) of each individual. Monitoring dives were performed monthly to check for the presence of the tagged sea urchins. Since the control areas are far from the CO_2 vents (4 and 40 km; Figure S1), we did not tag or follow the control animals.

Coelomic fluid sampling and analysis

For pH measurements, 1-2 ml of the coelomic fluid was collected by a hypodermic needle inserted into the perivisceral coelomic space through the peristomal membrane (n = 10 urchins from each site). The pH of the coelomic fluid was immediately (less than 10 s after extraction) measured in a 1.5 mL Eppendorf tube by immersing a pH probe (Beckman 511275-AB) in the fluid creating an anaerobic sealed area between the bottom of the tube and the tip of the pH probe. (Calosi et al., 2013a). The pH probe was connected to a pH meter

(Beckman 350). For other analyses 5-10 ml of the coelomic fluid were collected making a cut in the peristomal membrane by scissors, and poured on an equivalent amount of ice-cold 2× cell culture medium (CCM), composed of 1 M NaCl, 10 mM MgCl2, 40 mM Hepes, 2 mM EGTA pH 7.2 which is an anticoagulant solution (Pinsino et al., 2015). After collection in this solution, the immune cells were counted in a Fast-Read chamber (Biosigma) and a morphological analysis of viable cells was performed using an optical microscope (Leitz, Dialux 20 EB). The Trypan blue exclusion test was used to determine the number of viable cells present in the cell suspension as total cell population (Strober, 2001). The cell suspension was then centrifuged at 12000 g for 10 minutes. The cell-free supernatant was used to measure TA, PCO_2, $HCO_3^-$and CO_3^{2-} concentrations, ΩC and ΩA as described above. The pellet containing immune cells was washed in PBS and then deep-frozen in liquid nitrogen for further analyses.

Immune cell proteomics

The immune cell pellet was resuspended in 50 mM ammonium bicarbonate. Shotgun mass spectrometry and label free quantification was performed as described in Cocetti et al., 2008 . In detail, after reduction and derivatisation, the proteins were digested with trypsin sequence grade trypsin (Roche) for 16 h at 37 °C using a protein:trypsin ratio of 1:20 (Iametti, Tedeschi, Oungre, & Bonomi, 2001). Liquid chromatography-electrospray ionization-tandem mass spectrometry (LC-ESI-MS/MS) analysis was performed on a DionexUltiMate 3000 HPLC System with a PicoFritProteoPrep C18 column (200 mm, internal diameter of 75 µm) (New Objective, USA). Gradient: 1% Acetonitrile (ACN) in 0.1 % formic acid for 10 min, 1-4 % ACN in 0.1% formic acid for 6 min, 4-30% ACN in 0.1% formic acid for 147 min and 30-50 % ACN in 0.1% formic for 3 min at a flow rate of 0.3 µl/min. The eluate was electrosprayed into a linear quadrupole ion trap (LTQ) OrbitrapVelos (Thermo Fisher

Formattato: Non Evidenziato

Scientific, Bremen, Germany) through a Proxeon nano-electrospray ion source (Thermo Fisher Scientific). The LTQ-Orbitrap was operated in positive mode in data-dependent acquisition mode to automatically alternate between a full scan (m/z 350-2000) in the Orbitrap (at resolution 60000, AGC target 1000000) and subsequent Collision induced dissociation (CID) MS/MS in the linear ion trap of the 20 most intense peaks from full scan (normalized collision energy of 35%, 10 ms activation). Isolation window: 3 Da, unassigned charge states: rejected, charge state 1: rejected, charge states 2+, 3+, 4+: not rejected; dynamic exclusion enabled (60 s, exclusion list size: 200). Two biological replicates and four technical replicate analyses of each coelomocyte sample were performed. Data acquisition was controlled by Xcalibur 2.0 and Tune 2.4 software (Thermo Fisher Scientific).

Mass spectra were analysed using MaxQuant software (version 1.3.0.5). The initial maximum allowed mass deviation was set to 6 ppm for monoisotopic precursor ions and 0.5 Da for MS/MS peaks. Enzyme specificity was set to trypsin, defined as C-terminal to arginine and lysine excluding proline, and a maximum of two missed cleavages were allowed. Carbamidomethylcysteine was set as a fixed modification, N-terminal acetylation and methionine oxidation as variable modifications. The spectra were searched by the Andromeda search engine against the NCBI Sea_urchin sequence database. Protein identification required at least one unique or razor peptide per protein group. Quantification in MaxQuant was performed using the built in XIC-based label free quantification (LFQ) algorithm using fast LFQ. The required false positive rate was set to 1% at the peptide and 1% at the protein level, and the minimum required peptide length was set to 6 amino acids.

Formattato: Non Evidenziato

Nitric oxide determination in immune cells

The endogenous nitric oxide levels were measured by monitoring nitrite formation by Griess reaction. Immune cell pellets were mechanically homogenized in PBS buffer (1:2 w/v) and

centrifuged at 25,000 x g for 20 min at + 4°C. The supernatants were analyzed for nitrite content by Griess reagent (Migliaccio, Castellano, Romano, & Palumbo, 2014).

Lipid peroxidation in immune cells

Lipid peroxidation was measured by thiobarbituric acid method assay (TBA test), which is based on the reactivity of the end product of lipid peroxidation, the malondialdehyde (MDA) with TBA to produce a red adduct. Immune cell pellets were mechanically homogenized in Tris-HCl (1:2 w/v) and centrifuged (14,000 g for 30 min at 4°C). The supernatants were analyzed spectrophotmetrically for MDA content (Pagano et al., 2016).

Immune cells total antioxidant capacity

Total antioxidant capacity (TAC) was measured with a method based on the decolorization of 2,2′-azinobis-3-ethylbenzothiazoline-6-sulfonic acid (ABTS) radical cation (ABTS•+) by antioxidants in the samples (Re et al., 1999). Immune cells were suspended in phosphate buffer 50mM pH7.8 (1:2 w:v) and centrifuged at 14000 g for 30 min at 4°C, and the supernatant was used for the assay. The addition of the sample to the pre-formed radical ABTS, formed by the reaction of ABTS reacts with H_2O_2 in presence of horseradish peroxidase, induces ABTS reduction depending on antioxidant capacity. Thus, the extent of decolorization analyzed spectrophotmetrically, expressed as percentage inhibition of the ABTS•+ radical cation formation, is determined and compared with that of ascorbate assayed under the same experimental conditions (Re et al., 1999).

Animal respiration and nitrogen excretion

Respiration rates of sea urchins from control and acidified sites were tested at their respective pH conditions. Animals (10 per site) were collected, weighed, and transferred to glass

respiration chambers with a volume of 3L containing 0.2 µm filtered seawater collected from the investigated sites. Following acclimation (approximately 1h), respiration chambers were closed, and oxygen saturation was measured continuously (once every 15 s) for 2-3 hours at 18±2°C using oxygen microelectrode (YSI 5357 Micro Probe, USA), following the method described in Uliano et al., (2010). The decline in water oxygen concentration was approximately linear and oxygen consumption rates were calculated by linear regression analyses as reported in Uliano et al., (2010). The sensor was calibrated according to the manufacturer's instructions. A separate chamber was incubated without animals to determine background readings of filtered seawater for the respiration of bacteria. Oxygen consumption rates (rMO_2) are expressed as µmol O_2 g^{-1} h^{-1}.

At the beginning and at the end of each rMO_2 trial, samples of water were collected for successive evaluation of ammonia and urea excretion rate. For NH_4^+ determinations, a 25 µL sample and 100 µL of reagent containing orthophthaldialdehyde, sodium sulphite and sodium borate was added, as reported in Holmes et al. 1999. Samples were then incubated for 2.5 h at room temperature in the dark until fluorescence was determined at an excitation and emission wavelength of 360 and 422 nm, respectively, using a microplate reader (Molecular Device, Spectra Max, M5). Ammonia (NH_3) was not measured because its concentration is negligible at pH values of 8.0–7.1 (0.2–2% of total ammonium/ammonia; Korner et al., 2001). Urea concentration was determined colorimetrically using a diacetyl-monoxime method (modified from Rahmatullah & Boyde, 1980). In detail, urea was determined by a coupled enzymatic reaction, resulting in the formation of a coloured product absorbing at 525 nm analysed spectrophotmetrically. Ammonium and urea excretion rates (M_{amm} and M_{urea}, respectively) were expressed as µmol g^{-1} h^{-1}. The O:N ratio (oxygen consumed *versus* nitrogen excreted) was expressed as µmol N g^{-1} h^{-1} and was calculated as rMO_2/M_{Nw}, where M_{Nw} is the total waste nitrogen excretion rate ($M_{Nw}=M_{amm}+2\times M_{urea}$) (Mayzaud & Conover, 1988).

Mineralogy

X-ray diffractometry (XRD) was used to analyse the carbonate mineralogy (wt% $MgCO_3$) of six *Paracentrotus lividus* from each site. The tests were cleaned of internal organs, rinsed with distilled water, soaked in a mild bleach solution and dried at 60 °C for three days. For XRD, approximately 0.5g of each sample was placed in a clean mortar, with 0.1g of analytical grade halite (NaCl) as an internal standard, and ground to a fine powder until it was consistent in colour and texture. A small amount of 95% ethanol was added to make a slurry which was smeared uniformly on a glass slide and left to air dry. Each sample was scanned by a Phillips X-Ray diffractometer (XRD) between 26 and 33 °2θ. There was 1 count per degree, and the count time was 1 second. Calcite peak position was corrected based on the internal standard halite peak, and then a machine-specific calibration for determining Mg content was applied: $y = 30x - 882$, where y = wt% $MgCO_3$ in calcite and x = calcite peak position in °2θ (after Gray & Smith, 2004). For each urchin three spines and three test plates were analysed and the mean wt% $MgCO_3$ of the three measures was used as the independent datum for statistical analysis.

Statistical analyses

One -way ANOVA followed by Tukey's multiple comparisons test was utilized to assess the differences in immune cell counts and to analyze intracellular redox status of immune cells, and respiration rates and nitrogen excretion of animals. For the percent distribution of the different types of immune cells, arcsin transformation was applied to percentage values.

For protein data, statistical analyses were performed using the Perseus software (version 1.4.0.6, www.biochem.mpg.de/mann/tools/). Only proteins present and quantified in at least 3 out of 4 technical repeats were considered as positively identified in a sample and used for

statistical analyses. The protein data were analyzed by analysis of variance (ANOVA, FDR 0.05) to identify proteins differentially expressed among the different conditions. 311 proteins ANOVA significant were further analyzed focusing on the specific comparison between the data for the coelomic cells from the N2 and C1 urchins, the N2 and C2 urchins and those from C1 and C2. Proteins were considered differentially expressed if they were present only in one condition or showed significant difference (Welch test $p = 0.0167$). Bioinformatic analysis was carried out within the set of differentially expressed proteins ($p \leq 0.05$) by DAVID software (Huang, Sherman, & Lempicki, 2009a, 2009b) to cluster enriched annotation groups of molecular function, biological processes, biological cellular component, KEGG pathway, keywords and molecular complexes (CORUM). The mass spectrometry proteomics data have been deposited to the ProteomeXchange Consortium via the PRIDE (Vizcaíno et al., 2016) partner repository with the dataset identifier PXD009395. The mineralogy data for the wt% MgCO3 of the test and spines were analysed by one -way ANOVA. Homogeneity of variance was confirmed by Levene's test and normality was confirmed using Shapiro Wilks test.

Formattato: Non Evidenziato

Ethics statement

P. lividus from N2, C1 and C2 were collected from locations that are not privately-owned, and those from Ischia are included in sites in the Marine Protected Area "Regno di Nettuno", where the SZN has the authorization to collect marine organisms for research purposes. The field studies did not involve endangered or protected species. All animal procedures followed the guidelines of the European Union (directive 2010/63 and following D. Lgs. 4/03/2014 n. 26).

RESULTS

Sea urchins tagging from the N2 site

Paracentrotus lividus at the low-pH site (N2 site, pH 7.8) occur in burrows or crevices in the rocky reef and in the surrounding seagrass, *Posidonia oceanica* meadows at 1-3 m depth. The location of 50 tagged sea urchins was monitored monthly from August 2014 to February 2015 (Table S1), and of these, about 40% were identified throughout the 7 months. Some labels were lost in a storm in January 2015 preventing us to identify individuals, but this did not remove the sea urchins. Overall, the *P. lividus* at the N2 site exhibited site fidelity indicating a life time, long-term exposure to CO_2 vents conditions.

Coelomic fluid pH and immune cell count and morphology

The pH of the coelomic fluid of *P. lividus* from the three sites was ~ pH 7.6 (C1, pH = 7.56 ± 0.01; C2, pH = 7.59 ± 0.03; N2, pH = 7.62 ± 0.02; Table S2A) and did not differ indicating that their acid-base status was similar.

Three main types of circulating immune cells are present in the coelomic fluid of *P. lividus*, phagocytes, vibratile cells and amoebocytes with the latter including white and red amoebocytes (Fig. 1A). The total number of circulating immune cells did not differ between the vent and C1 site urchins (Fig. 1B, N2 *versus* C1; Table S2A), but the cell count for the urchins from the C2 site was higher than for the vent and the C1 site animals (Fig. 1B, C2 *versus* N2 and C2 *versus* C1; Table S2A).

There was no difference in the percentage of each immune cell type (red amoebocytes, white amoebocytes, vibratile cells and phagocytes) in urchins from the three sites (Fig. 1C) (Table S2B).

Proteomic analysis of immune cells

For proteomic analysis, a shotgun label free proteomic approach was carried out following the workflow described in Fig. 2A, which allowed obtaining a quantitative evaluation of the full proteome of the immune cells of sea urchins from the three sites. A total of 588 proteins were common to the immune cells of urchins across sites (Fig. 2A), 311 of which were found differentially expressed (listed in Table S3). As shown in the Venn diagram (Fig. 2B), the analysis indicates that a large proportion of the proteome is exclusive to urchins from individual sites, with 120, 103 and 105 proteins exclusively detected in C1, C2 and N2 samples, respectively.

The Volcano plots (Fig. S2) showed the differentially expressed proteins in each group of samples (Welch $p = 0.0167$) (see Tables S4, S5, S6, S7, S8, S9). Proteins were classified using DAVID ($p \leq 0.05$) (Table 1).

The comparison between the N2 and C1, and between the N2 and C2 urchins shows a significant enrichment in the dimethylaniline mono-oxygenase [N-oxide-forming] (IPR012143, Table 1, Table S4 and Table S6) and in the aldehyde dehydrogenase (LOC593236, Table 21, Table S4) in the vent urchins. The first is a flavin-containing mono-oxygenase (FMOs) important for the oxidative metabolism of a wide variety of natural and synthetic compounds. The second is an enzyme that catalyses the oxidation (dehydrogenation) of aldehydes and participates in a wide variety of biological processes including the detoxification of exogenously and endogenously generated aldehydes. Moreover, there is an enrichment of enzymes involved in oxidative processes that are differentially expressed in the immune cells of the vent urchins (N2 *vs* C1 and N2 vs C2; Fig. 3).

Overall, the proteomic profile indicates the general shift towards antioxidant processes in N2 samples, as revealed by the up-regulation of glutathione-S-transferase (gi|72160095;

Formattato: Non Evidenziato

Formattato: Non Evidenziato

Formattato: Non Evidenziato

gi|780075039, Table S4). On the other hand, lower production of reactive oxygen (ROS) and nitrogen species (RNS) was observed in immune cells of animals living at the vent site. Indeed, we observed an up-regulation of alternative oxidase mitochondrial-like (gi|780047432, Table S4; gi|780047432, Table S6) and a down-regulation of peroxiredoxin-5 (gi|779996132, Table S5), myeloperoxidase (gi|390346168, Table S5) and NADPH oxidase (gi|118601040, gi|390351201, Table S7). In agreement, levels of phagosome and microsomal proteins were higher in the immune cells of the sea urchins from the vent site, suggesting an increase in immune defense activity.

Regarding ammonium metabolism, the sea urchins living in the N2 site show an up-regulation of glutamate dehydrogenase (gi|780058304, Table S4; gi|780058366, Table S6), transglutaminase (gi|238776807, Table S6) and kynurenine--oxoglutarate transaminase 3 isoform X1 (gi|780156643, Table S6) and a down-regulation of carbamoyl-phosphate synthase (gi|780137773, Table S7). Moreover, the levels of enzymes involved in amino acid degradation, such as isovaleryl-CoA dehydrogenase (gi|780032420, Table S6) and 3-hydroxyisobutyrate dehydrogenase (gi|780122344, Table S6) were higher.

Levels of proteins involved in glycolysis/gluconeogenesis and in the pyruvate and propanoate metabolism were also higher in the vent urchin immune cells (Table 1). Indeed, Table 1 shows that N2 samples, compared to C1 presents modulation of many enzymes involved in the carbon metabolism KEGG pathway as shown in Fig. 4, namely up-regulation of the enzymes glutamate dehydrogenase mitochondrial (LOC584300) (1), acetyl-coenzyme A synthetase (LOC592086) (2), enoyl CoA hydratase (ECHS1) (3), glucose-6-phosphate isomerase (LOC762939) (4), acetyl-coenzyme A synthetase 2 (LOC585742) (5), and down-regulation of the enzymes malate dehydrogenase (LOC577019) (6), aspartate aminotransferase (LOC592180) (7), fructose-1,6-bisphosphatase 1 (LOC577064) (8),

succinyl-CoA ligase subunit alpha (LOC581456) (9), pyruvate kinase PKM (LOC592628) (10),.

Intracellular redox status of immune cells

Intracellular redox state of immune cells was evaluated by measuring lipid peroxidation and nitric oxide (NO) levels. Both parameters were similar between the N2 and control animals, indicating an absence of oxidative and nitrosative status in the immune cells (Fig. 5A, B, Table S2A). Interestingly, immune cells from the *P. lividus* living in the N2 zone exhibited a higher antioxidant capacity (TAC), compared to urchins from both control sites (Fig. 5C, Table S2A).

Respirometry and nitrogen excretion

The metabolic rate, rMO_2, of *P. lividus* ranged from 0.25 to 0.27 μmol $O_2\ g^{-1}\ h^{-1}$ and did not differ in urchins from the three sites (Table S10, Table S2A). Nitrogen excretion rates (M_{amm}, M_{urea} and M_{Nw}) were slightly higher in the C2 site urchins compared to those from C1 and N2 (Table S10), but this was not significant (Table S2A). Consequently, the O:N ratio also did not differ in the urchins from the different sites (Table S10, Table S2A).

Mineralogy

There was no difference in the % $MgCO_3$ in the spine ($p = 0.36$) and test ($p = 0.70$) skeleton of *P. lividus* from vent and control sites (Table S11, Table S2A). The urchins from all sites were similar in having a significantly higher percentage of $MgCO_3$ in the test (mean 9.0 wt% $MgCO_3$; ± 0.13 SE, n = 18) compared with the spines (mean 3.09 wt% $MgCO_3$, ± 0.13 SE, n = 18).

DISCUSSION

In this study, we examined the immune system of echinoderms living at low pH/high pCO_2, defining the metabolic pathway(s) that have allowed long-term adaptation/acclimatisation of *Paracentrotus lividus* to OA. This species is the most common macroinvertebrate living at the Castello Aragonese volcanic CO_2 vents at the pH 7.8 zone and in nearby rocky reefs in control areas (Kroeker et al., 2013a). Indeed, the animals remained at the same spot over 6-7 months, as revealed by tagging experiments, in accordance with a previous study showing that *P. lividus* was observed at the vent N2 site for 3 years (Kroeker et al., 2013a).

The novelty of the present study is the analysis of the sea urchin immune cells by a wide-ranging approach, which included cell morphology, biochemistry and proteomics. In particular, it's the first time that proteomics technology has been applied to investigate the changes in immune cells proteome in a natural population of animals resident in low pH/high pCO_2 conditions. Up to now, few proteomic studies have been performed only in laboratory experiments and not on immune cells. The pathways affected by OA have been identified by proteomics in gills or mantle tissues of oysters exposed at different pCO_2 levels (Goncalves, Thompson, & Raftos, 2017; Timmins-Schiffman et al., 2014; Tomanek, Zuzow, Ivanina, Beniash, & Sokolova, 2011).

As sentinels of environmental stress responses, the number and types of sea urchin immune cells have been mainly examined up to now for the activation/inactivation of the cellular stress responses (Pinsino & Matranga, 2015). The immune cells of *P. lividus* living at the vent site did not exhibit any differences in the percentage of each immune cell compared to control site urchins. However, the number of circulating cells in the N2 urchins was similar to that from control zone C1 at Ischia island, but lower compared to the control C2 urchins. The high number of immune cells found in C2, a site close to the urban area of Naples, was likely due to unknown sources of stress absent in the proximity of Ischia island.

The significant enrichment of oxidative processes observed at proteomic level in immune cells in sea urchins at low-pH zone is counteracted by the enhancement of the total antioxidant activity, as also supported by the proteomic profile, indicating a general shift towards antioxidant processes in the vent urchins. The effectiveness of the antioxidant response resulted in the absence of any changes in the oxidative and nitrosative status of the immune cells in sea urchins living at low-pH zone. Interestingly, coelomocytes exhibit total antioxidant capacity much higher than that of the other tissues, possibly related to the lifespan of the sea urchin species (Du, Anderson, Lortie, Parsons, & Bodnar, 2013). The antioxidant response in the vent urchin coelomic cells represents a general cellular protective mechanism which is used to balance stress conditions, as reported in gonad of *P. lividus* fed with invasive algae (Tejada, Deudero, Box, & Sureda, 2013) or in mantle tissue of oysters as response to elevated $pPCO_2$ levels (Tomanek et al., 2011). The up-regulation of antioxidant systems is also adopted by sea urchin larvae in response to natural levels of UV-B radiation (Lister, Lamare, & Burritt, 2010). In addition, sea urchin embryos have been reported to produce the potent antioxidant ovotiol to counteract the stress induced by metal ions and toxic blooms (Castellano et al., 2016).

The finding that the coelomic fluid of the vent urchins was pH 7.6 is similar to that previously reported for *P. lividus* and other sea urchin species (Calosi et al., 2013a; Collard et al., 2013; Dwoarjanyn & Byrne, 2018; Lewis et al., 2016; Uthicke et al., 2014). Coelomic pH did not differ between control and acidified conditions as also shown in a previous comparison of vent and control site urchins as well as in laboratory OA studies at similar pH levels (Calosi et al., 2013a; Catarino et al., 2012; Lewis et al., 2016; Uthicke et al., 2014). These findings show that sea urchins are steady regulators of the coelomic fluid acid-base balance. In this aspect, they differ from bivalves which are poor regulators of the haemolymph acid-base balance. Indeed, seawater acidification induced immune function

changes of haemocytes in *Mytilus edulis* with increases in ROS production and antioxidant components (Sun, Tang, Jiang, & Wanga, 2017).

Another important finding from the proteomics is the increased ammonium metabolism in the immune cells harvested from urchins resident in low-pH conditions. This is seen in the higher levels of glutamate dehydrogenase, transglutaminase and kynurenine-oxoglutarate transaminase 3 isoform X1 and lower levels of the first enzyme of the urea cycle carbamoyl-phosphate synthase in the immune cell proteome from the vent urchins. Supporting evidence is the increased levels of several enzymes, including isovaleryl-CoA dehydrogenase and 3-hydroxyisobutyrate dehydrogenase, which are involved in aminoacid degradation. However, this result was not reflected in the whole-body ammonia production, as there was no significant difference in the nitrogen excretion rates of urchins from the three sites.

Interestingly, the lack of differences in GSI, animal size as well as in major physiological parameters, including acid-base balance respiration and nitrogen excretion, compared to control site animals indicates physiological adaptation to life at the vent. This is similar to that found for an *Echinometra* species resident at the vents at Papua New Guinea at similar conditions (pH 7.76) (Uthicke et al., 2016).

Many studies highlight the effects of OA on marine calcifiers from a range of marine ecosystems, demonstrating the potential for deleterious effects on calcification (Kreoeker …). Echinoderms have skeletons formed of high-magnesium calcite (mean 7.5, range 1 to 16wt % $MgCO_3$) (Dubois, 2014; Smith, Clark, Lamare, Winter, & Byrne, 2016), the mineral state considered most vulnerable to dissolution due to CO_2-driven OA (McClintock et al., 2011; Morse, Andersson, & Mackenzie, 2006). This potential vulnerability might in part be limited by a protective epithelial and extracellular cuticle cover (see Dubois, 2014). Our finding that CO_2-driven acidification (pH 7.8) does not affect the $MgCO_3$ content of the skeleton of *P. lividus* is in line with recent long-term laboratory experiments (Byrne et al., 2014; Ries, 2011;

Ries, Cohen, & McCorkle, 2009) as well as with studies on *Tripneustes gratilla* where the urchins were reared from the juvenile to the large mature adult in OA conditions (Byrne et al., 2014).

CONCLUSIONS

Our data indicate the great potential of *P. lividus* to acclimatize/adapt to near future OA conditions by altering the metabolism of immune cells through a rearrangement of defensive abilities, and in particular antioxidant processes. This indicates a phenotypic plasticity of the sea urchin coelomic and immune systems to adjust their defensive and homeostatic responses, an ability that will likely be a key trait to persist in climate driven changes in ocean conditions.

ACKNOWLEDGEMENTS

This paper is dedicated to the memory of Valeria Matranga who contributed significantly to the understanding of how sea urchin immune cells can be employed to evaluate environmental changes. She and her insight for creative approaches in eco-immuno-toxicology will be missed. Oriana Migliaccio acknowledges the award she received, in the frame of Summer Program in Taiwan for Italian Graduate Students(MOST), to work for two months in 2016 in the laboratory of Prof. Yung-Che Tseng, National Taiwan Normal University, to increase her physiological knowledge.

FUNDING

This work was partially supported from SZN funds, the European Union's Horizon 2020 research and innovation program under the Marie Skłodowska-Curie grant agreement No 67188 (IBIM-CNR Unit). Oriana Migliaccio was supported by a SZN PhD fellowship.

AUTHORS' CONTRIBUTION

OM, MCG, AP conceived and designed the experiments. OM, APi, EM, SN, AS, GT, MCG performed the experiments. OM, APi, CA, GT, MB, MCG, AP analyzed the data. APi, GT, MB, MCG, AP provided reagents, materials and analysis tools. OM, CA, MB, MCG, AP drafted the paper. All authors revised and approved the final manuscript.

Formattato: Non Evidenziato

REFERENCES

Albright, R., Caldeira, L., Hosfelt, J., Kwiatkowski, L., Maclaren, J. K., Mason, B. M., . . . Caldeira, K. (2016). Reversal of ocean acidification enhances net coral reef calcification. *Nature*, 531, 362-365. DOI: 10.1038/nature17155

Barry, J. P., Lovera, C., Buck, K. R., Peltzer, E. T., Taylor, J. R., Walz, P., . . . Brewer, P. G. (2014). Use of a free ocean CO_2 enrichment (FOCE) system to evaluate the effects of ocean acidification on the foraging behavior of a deep-sea urchin. *Environmental Science & Technology*, 48, 9890-9897. DOI: 10.1021/es501603r

Barry, J. P., Hall-Spencer, J. M., & Tyrrell, (2010). *In situ* perturbation experiments: natural venting sites, spatial/temporal gradients in ocean pH, manipulative *in situ* pCO_2 perturbations. In: U. Riebesell, V. J. Fabry, L. Hansson & J. P. Gattuso (Eds.), *Guide to best practices for ocean acidification research and data reporting* (Chapter 8, pp. 123 – 136). Luxembourg: Publications Office of the European Union

Bodnar, A. G. (2013). Proteomic profiles reveal age-related changes in coelomic fluid of sea urchin species with different life spans. *Experimental Gerontology* 48, 525–530. DOI: 10.1016/j.exger.2013.01.014

Bögner, D. (2016). Life under Climate Change Scenarios: Sea urchins' cellular mechanisms for reproductive success. *Journal of Marine Science and Engineering*, 4, 28. https://doi.org/10.3390/jmse4010028

Boudouresque, C. F., & Verlaque, M. (2013). Paracentrotus lividus. In: J. M. Lawrence (Ed.), *Sea Urchins: Biology and Ecology*, Third Edition (pp. 297-327). Elsevier

Brothers, C. J., Harianto, J., McClintock, J. B., & Byrne, M. (2016). Sea urchins in a high-CO2 world: the influence of acclimation on the immune response to ocean warming and acidification. *Proceedings of the Royal Society B*, 283, 20161501. DOI: 10.1098/rspb.2016.1501

Bulleri, F., Benedetti-Cecchi, L., & Cinelli, F. (1999). Grazing by the sea urchins Arbacia lixula L. and Paracentrotus lividus Lam. in the Northwest Mediterranean. *Journal of Experimental Marine Biology and Ecology*, 241, 81-95. https://doi.org/10.1016/S0022-0981(99)00073-8

Burnell, O., Russell, B., Irving, A., & Connell, S. (2013). Eutrophication offsets increased sea urchin grazing on seagrass caused by ocean warming and acidification. *Marine Ecology Progress Series*, 485, 37-46. https://doi.org/10.3354/meps10323

Byrne, M., Smith, A. M., West, S., Collard, M., Dubois, P., Graba-landry, A., & Dworjanyn, S. A. (2014). Warming Influences Mg(2+) content, while warming and acidification influence calcification and test strength of a sea urchin. *Environmental Science & Technology*, 48, 12620-12627. DOI: 10.1021/es5017526

Byrne, M., Lamare, M., Winter, D., Dworjanyn, S. A., & Uthicke, S. (2013). The stunting effect of a high CO_2 ocean on calcification and development in sea urchin larvae, a synthesis from the tropics to the poles. *Philosophical Transactions of the Royal Society B*, 368, 20120439. DOI: 10.1098/rstb.2012.0439

Calosi, P., Rastrick, S. P. S., Graziano, M., Thomas, S. C., Baggini, C., Carter, H. A, . . . Spicer JI. (2013a). Distribution of sea urchins living near shallow water CO_2 vents is dependent upon species acid-base and ion-regulatory abilities. *Marine Pollution Bulletin*, 73, 470-484. https://doi.org/10.1016/j.marpolbul.2012.11.040

Calosi, P., Rastrick, S. P. S., Lombardi, C., de Guzman, H. J., Davidson, L., Jahnke, M., . . . Gambi, M. C. (2013b). Adaptation and acclimatization to ocean acidification in marine ectotherms: an in situ transplant experiment with polychaetes at a shallow CO2 vent system. *Philosophical Transactions of the Royal Society B*, 368, 20120444. http://dx.doi.org/10.1098/rstb.2012.0444

Carey, N., Harianto, J., & Byrne, M. (2016). Sea urchins in a high-CO2 world: partitioned effects of body size, ocean warming and acidification on metabolic rate. *Journal of Experimental Biology*, 219, 1178-1186. DOI: 10.1242/jeb.136101

Castellano, I., Migliaccio, O., D'Aniello, S., Merlino, A., Napolitano, A., & Palumbo, A. (2016). Shedding light on ovothiol biosynthesis in marine metazoans. *Scientific Reports*, 6, 21506. DOI: 10.1038/srep21506

Catarino, A. I., Bauwens, M., & Dubois, P. (2012). Acid-base balance and metabolic response of the sea urchin *Paracentrotus lividus* to different seawater pH and temperatures. *Environmental Science and Pollution Research*, 19, 2344-2353. DOI: 10.1007/s11356-012-0743-1

Coccetti, P., Tripodi, F., Tedeschi, G., Nonnis, S., Marin, O., Fantinato, S., . . . Alberghina, L. (2008). The CK2 phosphorylation of catalytic domain of Cdc34 modulates its activity at the G1 to S transition in Saccharomyces cerevisiae. *Cell Cycle, 7*(10), 1391-1401. doi:10.4161/cc.7.10.5825

Formattato: Non Evidenziato

Collard, M., Rastrick, S. P. S., Calosi, P., Demolder, Y., Dille, J., Findlay, H. S., . . . Dubois, P. (2016). The impact of ocean acidification and warming on the skeletal mechanical properties of the sea urchin *Paracentrotus lividus* from laboratory and field observations. ICES Journal of Marine Science, 73, 727-738. doi:10.1093/icesjms/fsv018

Collard, M., Laitat, K., Moulin, L., Catarino, A. I., Grosjean, P., & Dubois, P. (2013). Buffer capacity of the coelomic fluid in echinoderms. *Comparative Biochemistry and Physiology - Part A: Molecular & Integrative Physiology*, 166, 199-206. DOI: 10.1016/j.cbpa.2013.06.002

Connell, S. D., Kroeker, K. J., Fabricius, K. E., Kline, D. I., & Russell, B. D. (2013). The other ocean acidification problem: CO2 as a resource among competitors for ecosystem dominance. *Philosophical Transactions of the Royal Society B*, 368, 20120442. DOI: 10.1098/rstb.2012.0442

Doney, S. C., Ruckelshaus, M., Duffy, J. E., Barry, J. P., Chan, F., English, C. A., . . . Talley, L. D. (2012). Climate change impacts on marine ecosystems. *Annual Review of Marine Science*, 4, 11-37. DOI: 10.1146/annurev-marine-041911-111611

Du, C., Anderson, A., Lortie, M., Parsons, R., Bodnar, A. (2013). Oxidative Damage and Cellular Defense Mechanisms in Sea Urchin Models of Aging. *Free Radical Biology & Medicine*, 63, 254–263. DOI: 10.1016/j.freeradbiomed.2013.05.023

Dubois, P. (2014). The skeleton of postmetamorphic echinoderms in a changing world. *The Biological Bulletin*, 226, 223-236. DOI: 10.1086/BBLv226n3p223

Dworjanyn, S. A. & Byrne, M. (2018). Impacts of ocean acidification on sea urchin growth across the juvenile to mature adult life-stage transition is mitigated by warming. *Proceedings of the Royal Society B*, 285, 20172684. https://doi.org/10.1098/rspb.2017.2684

Foo, S. A., Byrne, M., Ricevuto, E., & Gambi, M. C. (2018). The carbon dioxide vents of Ischia, Italy, a natural laboratory to assess impacts of ocean acidification on marine ecosystems: an overview of research and comparisons with other vent systems. In S. J. Hawkins, A. J. Evans, A. C. Dale, L. B. Firth, D. J. Hughes & I. P. Smith (Eds.), *Oceanography and Marine Biology. An Annual Review*, in press. Boca Raton: CRC Press

Garrard, S. L., Hunter, R. C., Frommel, A. Y., Lane, A. C., Phillips, J. C., Cooper, . . . Bjoerk, M. M. (2012). Biological impacts of ocean acidification: a postgraduate perspective on research priorities. *Marine Biology*, 160, 1789-1805. DOI: 10.1007/s00227-012-2033-3

Gattuso, J. P., Magnan, A., Billé, R., Cheung, W. W., Howes, E. L., Joos, F., . . . Turley C. (2015). Oceanography. Contrasting futures for ocean and society from different anthropogenic CO_2 emissions scenarios. *Science*, 349, aac4722. DOI: 10.1126/science

Goncalves, P., Thompson, E. L., & Raftos, D. A. (2017). Contrasting impacts of ocean acidification and warming on the molecular responses of CO_2-resilient oysters. *BMC Genomics*, 18, 431. DOI 10.1186/s12864-017-3818-z

Gray, B. E. & Smith, A. M. (2004). Mineralogical variation in shells of the blackfoot abalone Haliotis iris (Mollusca: Gastropoda: Haliotidae), in southern New Zealand. *Pacific Science*, 58: 47−64. DOI: 10.1353/psc.2004.0005

Guidetti, P., & Mori, M, (2005). Morpho-functional defences of Mediterranean sea urchins, *Paracentrotus lividus* and *Arbacia lixula*, against fish predators. *Marine Biology*, 147, 797-802. DOI: 10.1007/s00227-005-1611-z

Hall-Spencer, J. M., Rodolfo-Metalpa, R., Martin, S., Ransome, E., Fine, M., Turner, S. M., . . . Buia, M. C. (2008). Volcanic carbon dioxide vents show ecosystem effects of ocean acidification. *Nature*, 454, 96-99. DOI:10.1038/nature07051

Holmes, R. M., Aminot, A., Kérouel, R., Hooker, B. A., & Peterson, B. J. (1999). A simple and precise method for measuring ammonium in marine and freshwater ecosystems. *Canadian Journal of Fisheries and Aquatic Sciences*, 56, 1801-1808.

Huang, D. W., Sherman, B. T., & Lempicki, R. A. (2009a). Systematic and integrative analysis of large gene lists using DAVID Bioinformatics Resources. *Nature Protocols*, 4, 44-57. DOI: 10.1038/nprot.2008.211

Huang, D. W., Sherman, B. T., & Lempicki, R. A. (2009b). Bioinformatics enrichment tools: paths toward the comprehensive functional analysis of large gene lists. *Nucleic Acids Research*, 37, 1-13. DOI: 10.1093/nar/gkn923.

Iametti, S., Tedeschi, G., Oungre, E., & Bonomi, F. (2001). Primary structure of kappa-casein isolated from mares' milk. *Journal of Dairy Research*, 68, 53-61.

IPCC (2014). Climate Change 2014: Synthesis Report. Contribution of Working Groups I, II and III to the Fifth Assessment Report of the Intergovernmental Panel on Climate Change. In R. K. Pachauri & L. A. Meyer (Eds.). Geneva, Switzerland, IPCC, 151 pp.

Kroeker, K. J., Micheli, F., & Gambi, M. C. (2013a). Ocean acidification causes ecosystem shifts via altered competitive interactions. *Nature Climate Change*, 3, 156-159. DOI: 10.1038/NCLIMATE1680

Kroeker, K. J., Gambi, M. C., & Micheli, F. (2013b) Community dynamics and ecosystem simplification in a high-CO2 ocean. *Proceedings of the National Academy of Sciences of the United States of America*, 110, 12721-12726. https://doi.org/10.1073/pnas.1216464110

Kroeker, K. J., Micheli, F., Gambi, M. C., & Martz, T. R. (2011). Divergent ecosystem responses within a benthic marine community to ocean acidification. *Proceedings of the National Academy of Sciences of the United States of America*, 108, 14515–14520. https://doi.org/10.1073/pnas.1107789108

Kroeker, K. J., Kordas, R. L., Crim, R. N., & Singh, G. G. (2010). Meta-analysis reveals negative yet variable effects of ocean acidification on marine organisms. *Ecology Letters*, 13, 1419-1434. https://doi.org/10.1111/j.1461-0248.2010.01518.x

Kurihara, H., Yin, R., Nishihara, G. N., Soyano, K., & Ishimatsu, A. (2013). Effect of ocean acidification on growth, gonad development and physiology of the sea urchin *Hemicentrotus pulcherrimus*. *Aquatic Biology*, 18, 281-292. DOI: 10.3354/ab00510

Lewis, C., Ellis, R. P., Vernon, E., Elliot, K., Newbatt, S., & Wilson, R. W. (2016). Ocean acidification increases copper toxicity differentially in two key marine invertebrates with distinct acid-base responses. *Scientific Reports*, 6, 21554. DOI: 10.1038/srep21554

Lister, K. N., Lamare, M. D., & Burritt, D.J. (2010). Oxidative Damage in Response to Natural Levels of UV-B Radiation in Larvae of the Tropical Sea Urchin *Tripneustes gratilla*. *Photochemistry and Photobiology*, 86, 1091–1098. DOI: 10.1111/j.1751-1097.2010.00779.x

Matranga, V., Toia, G., Bonaventura, R., & Müller, W. E. (2000). Cellular and biochemical responses to environmental and experimentally induced stress in sea urchin coelomocytes. *Cell Stress Chaperones*, 5, 113-120.

Mayzaud, P., & Conover, R. J. (1988). O:N ratio as a tool to describe zooplankton metabolism. *Marine Ecology Progress Series*, 45, 289-302.

McClintock, J. B., Amsler, M. O., Angus, R. A., Challener, R. C., Schram, J. B., Amsler, . . . Baker, B. J. (2011). The Mg-Calcite composition of Antarctic echinoderms: important implications for predicting the impacts of ocean acidification. *The Journal of Geology*, 119, 457-466. https://doi.org/10.1086/660890

Migliaccio, O., Castellano, I., Di Cioccio, D., Tedeschi, G., Negri, A., Cirino, P., . . . Palumbo, A. (2016). Subtle reproductive impairment through nitric oxide-mediated

mechanisms in sea urchins from an area affected by harmful algal blooms. *Scientific Reports*, 6, 26086. DOI: 10.1038/srep26086

Migliaccio, O., Castellano, I., Romano, G., & Palumbo, A. (2014). Stress response to cadmium and manganese in *Paracentrotus lividus* developing embryos is mediated by nitric oxide. *Aquatic Toxicology*, 156, 125-134. DOI: 10.1016/j.aquatox.2014.08.007

Morroni, L., Pinsino, A., Pellegrini, D., Regoli, F., & Matranga, V. (2016). Development of a new integrative toxicity index based on an improvement of the sea urchin embryo toxicity test. *Ecotoxicology and Environmental Safety*, 123, 2-7. https://doi.org/10.1016/j.ecoenv.2015.09.026

Morse, J. W., Andersson, A. J., & Mackenzie, F. T. (2006). Initial responses of carbonate-rich shelf sediments to rising atmospheric pCO_2 and "ocean acidification": Role of high Mg-calcites. *Geochimica et Cosmochimica Acta*, 70, 5814-5830. https://doi.org/10.1016/j.gca.2006.08.017

Nogueira, P., Gambi, M. C., Vizzini, S., Califano, G., Tavares, A. M., Santos, R., & Martinez-Crego, B. (2017). Altered epiphyte community and sea urchin diet in Posidonia oceanica meadows in the vicinity of submarine volcanic CO_2 vents. *Marine Environmental Research*, 127, 102-111. DOI: 10.1016/j.marenvres.2017.04.002.

Pagano, G., Guida, M., Siciliano, A., Oral, R., Koçbaşc, F., Palumbo A, . . . Trifuoggi M. (2016). Comparative Toxicities of Selected Rare Earth Elements: Sea Urchin Embryogenesis and Fertilization Damage with Redox and Cytogenetic Effects. *Environmental Research*, 147, 453–460. DOI: 10.1016/j.envres.2016.02.031

Pinsino, A., & Matranga, V. (2015). Sea urchin immune cells as sentinels of environmental stress. *Developmental Comparative Immunology*, 49, 198-205. DOI: 10.1016/j.dci.2014.11.013

Pinsino, A., Russo, R., Bonaventura, R., Brunelli, A., Marcomini, A., & Matranga, V. (2015) Titanium dioxide nanoparticles stimulate sea urchin immune cell phagocytic activity involving TLR/p38 MAPK-mediated signalling pathway. *Scientific Reports*, 5, 14492. DOI: 10.1038/srep14492

Pinsino, A., Della Torre, C., Sammarini, V., Bonaventura, R., Amato, E., & Matranga, V. (2008). Sea urchin coelomocytes as a novel cellular biosensor of environmental stress: a field study in the Tremiti Island Marine Protected Area, Southern Adriatic Sea, Italy. *Cell Biology and Toxicology*, 24, 541-552. DOI 10.1007/s10565-008-9055-0

Przeslawski, R., Byrne, M., & Mellin, C. (2015). A review and meta‐analysis of the effects of multiple abiotic stressors on marine embryos and larvae. *Global Change Biology*, 21, 2122-2140. doi: 10.1111/gcb.12833

Rahmatullah, M., & Boyde, T. R. (1980). Improvements in the determination of urea using diacetyl monoxime; methods with and without deproteinisation. *Clinica Chimica Acta*, 107, 3-9. DOI: 10.1016/j.cbpa.2010.07.019

Re, R., Pellegrini, N., Proteggente, A., Pannala, A., Yang, M., & Rice Evans, C. (1999). Antioxidant activity applying an improved ABTS radical cation decolorization assay. *Free Radical Biology & Medicine*, 26,1231–1237. https://doi.org/10.1016/S0891-5849(98)00315-3

Ricevuto, E., Kroeker, K. J., Ferrigno, F., Micheli, F., & Gambi, M. C. (2014). Spatio-temporal variability of polychaete colonization at volcanic CO2 vents indicates high tolerance to ocean acidification. *Marine Biology*, 161, 2909-2919. DOI: 10.1007/s00227-014-2555-y

Ries, J. B. (2011). Skeletal mineralogy in a high-CO_2 world. *Journal of Experimental Marine Biology and Ecology*, 403, 54-64. https://doi.org/10.1016/j.jembe.2011.04.006

Ries, J. B., Cohen, A. L., & McCorkle, D. C. (2009). Marine calcifiers exhibit mixed responses to CO2-induced ocean acidification. *Geology*, 37, 1131-1134. https://doi.org/10.1130/G30210A.1

Sala, E., Ribes, M., Hereu, B., Zabalal, M., Alva, V., Coma, R., & Garrabou, J. (1998). Temporal variability in abundance of the sea urchins *Paracentrotus lividus* and *Arbacia lixula* in the northwestern Mediterranean: comparison between a marine reserve and an unprotected area. *Marine Ecology Progress Series*, 168, 135-145.

Smith, A. M., Clark, D. E., Lamare, M., D., Winter, D. J., & Byrne, M., (2016). Risk and Resilience: variations in magnesium in echinoid skeletal calcite. *Marine Ecology Progress Series*, 561, 1-16. https://doi.org/10.3354/meps11908

Strober, W. (2001). Trypan blue exclusion test of cell viability. *Current Protocols in Immunology*, Appendix3:Appendix B. https://doi.org/10.1002/0471142735.ima03bs21

Stumpp, M., Trübenbach, K., Brennecke, D., Hu, M. Y., & Melzner, F. (2012). Resource allocation and extracellular acid-base status in the sea urchin *Strongylocentrotus droebachiensis* in response to CO_2 induced seawater acidification. *Aquatic Toxicology*, 110-111, 194-207. DOI: 10.1016/j.aquatox.2011.12.020.

Sun, T., Tang, X., Jiang, Y., & Wanga, Y. (2017). Seawater acidification induced immune function changes of haemocytes in *Mytilus edulis*: a comparative study of CO_2 and HCl enrichment. *Scientific Reports*, 7, 41488. DOI: 10.1038/srep41488

Tarasov, V. G. (2006). Effects of shallow-water hydrothermal venting on biological communities of coastal marine ecosystems of the Western Pacific. *Advances in Marine Biology*, 6, 267-421. https://doi.org/10.1016/S0065-2881(05)50004-X

Formattato: Italiano

Tedesco, D. (1996). Chemical and isotopic investigations of fumarolic gases from Ischia Island (Italy): Evidence of magmatic and crustal contribution. *Journal of Volcanology and Geothermal Research*, 74, 233–242. https://doi.org/10.1016/S0377-0273(96)00030-3

Tejada, S., Deudero, S., Box, A., & Sureda, A. (2013). Physiological response of the sea urchin *Paracentrotus lividus* fed with the seagrass *Posidonia oceanica* and the alien algae *Caulerpa racemosa* and *Lophocladia lallemandii*. *Marine Environmental Research*, 83: 48-53. DOI: 10.1016/j.marenvres.2012.10.008

Timmins-Schiffman, E., Coffey, W. D., Hua, W., Nunn, B. L., Dickinson, G. H., & Roberts, S. B. (2014). Shotgun proteomics reveals physiological response to ocean acidification in *Crassostrea gigas* Pacific oyster. *BMC Genomics*, 15:951. DOI: 10.1186/1471-2164-15-951

Tomanek, L., Zuzow, M. J., Ivanina, A. V., Beniash, E., & Sokolova, I. M. (2011). Proteomic response to elevated PCO_2 level in eastern oysters, *Crassostrea virginica*: evidence for oxidative stress. *Journal of Experimental Biology*, 214, 1836-1844. DOI: 10.1242/jeb.055475

Uliano, E., Cataldi, M., Carella, F., Migliaccio, O., Iaccarino, D., & Agnisola, C. (2010). Effects of acute changes in salinity and temperature on routine metabolism and nitrogen excretion in gambusia (*Gambusia affinis*) and zebrafish (*Danio rerio*). *Comparative Biochemistry and Physiology - Part A: Molecular & Integrative Physiology*, 157, 283-290. DOI: 10.1016/j.cbpa.2010.07.019

Uthicke, S., Ebert, T., Liddy, M., Johansson, C., Fabricius, K. E., & Lamare, M. (2016). Echinometra sea urchins acclimatised to elevated pCO_2 at volcanic vents outperform those under present-day pCO_2 conditions. *PANGAEA*, https://doi.org/10.1594/PANGAEA.864044

Formattato: Italiano

Formattato: Italiano

Formattato: Italiano

Uthicke, S., Liddy, M., Nguyen, H. D., & Byrne, M. (2014). Interactive effects of near-future temperature increase and ocean acidification on physiology and gonad development in adult Pacific sea urchin, *Echinometra* sp. *A*. *Coral Reefs*, 33, 831–845. DOI: 10.1007/s00338-014-1165-y

Uthicke, S., Soars, N., Foo, S., & Byrne, M. (2013). Physiological effects of increased pCO_2 and the effect of parent acclimation on development in the tropical Pacific sea urchin *Echinometra mathaei*. *Marine Biology*, 160, 1913-1926. DOI: 10.1007/s00227-012-2023-5

Vizcaíno, J. A., Csordas, A., del-Toro, N., Dianes, J. A., Griss, J., Lavidas, I., . . . Hermjakob, H. (2016). 2016 update of the PRIDE database and related tools. *Nucleic Acids Research*, 44, D447-456. DOI: 10.1093/nar/gkv1145

Vizzini, S., Di Leonardo, R., Costa, V., Tramati, C. D., Luzzu, F., & Mazzola, A. (2013). Trace element bias in the use of CO_2 vents as analogues for low pH environments: Implications for contamination levels in acidified oceans. *Estuarine, Coastal and Shelf Science*, 134, 19-30, https://doi.org/10.1016/j.ecss.2013.09.015

Formattato: Italiano

FIGURE LEGENDS

Figure 1 Immune cells in *Paracentrotus lividus*. (A) Morphology of immune cells in *Paracentrotus lividus*: phagocytes (black arrows); red amoebocytes (red arrows); white/colourless amoebocytes (white arrows) and vibratile cells (blue arrows). (B) Total immune cells count and (C) percent distribution of cell types in sea urchins collected at N2 and control sites C1 and C2. Bars represent mean ± SE (n = 10). *a*, significant difference between C1 and C2 (P<0.0001); *b*, significant difference between C2 and N2 (P<0.001) (one-way ANOVA and Tukey's post hoc test, see Table S2). Bars represent mean ± SE (n = 10). ra= red amoebocytes, wa = white amoebocytes, vc= vibratile cells, p= phagocytes.

Figure 2 Proteomic workflow and Venn diagram comparing the proteome of the immune cells from N2, C1 and C2 sea urchins. (A) Shotgun proteomic analysis was performed on sea urchins proteome from C1, C2 and N2 sites. Statistical analyses were performed using the Perseus software (version 1.4.0.6, www.biochem.mpg.de/mann/tools/). (B) Venn diagram showing the individual and shared proteins in sea urchins across sites. Only proteins present and quantified in at least 6 out of 8 repeats were considered as positively identified in a sample and used for statistical analyses.

Formattato: Inglese (Stati Uniti)

Formattato: Inglese (Stati Uniti), Non Evidenziato

Formattato: Non Evidenziato

Figure 3 Pie charts of the number of enzymes involved in oxidative processes, which are differentially expressed in immune cells from N2, C1 and C2 sea urchins. Numbers next to the red sections refer to the protein category count.

Figure 4 Carbon metabolism: the enzymes up or down-regulated in immune cells in a comparison N2 *versus* C1 are indicated by red stars. 1, glutamate dehydrogenase mitochondrial; 2, acetyl-coenzyme A synthetase; 3, enoyl CoA hydratase; 4, glucose-6-phosphate isomerase; 5, acetyl-coenzyme A synthetase 2; 6, malate dehydrogenase; 7, aspartate aminotransferase; 8, fructose-1,6-bisphosphatase 1; 9, succinyl-CoA ligase subunit alpha; 10, pyruvate kinase.

Figure 5 Intracellular redox state in immune cells of urchins from the three sites (A) Lipid peroxidation, (B) NO production and (C) Antioxidant defense. Bars represent mean ± SE (n = 10). *a*, significant difference between C1 and C2 (P<0.01); *b*, significant difference C1 and N2 (P<0.0001); c, significant difference C2 and N2 (P<0.05) (one-way ANOVA and Tukey's post hoc test, see details in Table S2A). Bars represent mean ± SE (n = 6 in A, B and C).

SUPPORTING INFORMATION

Additional Supporting Information may be found online in the supporting information tab for this article.

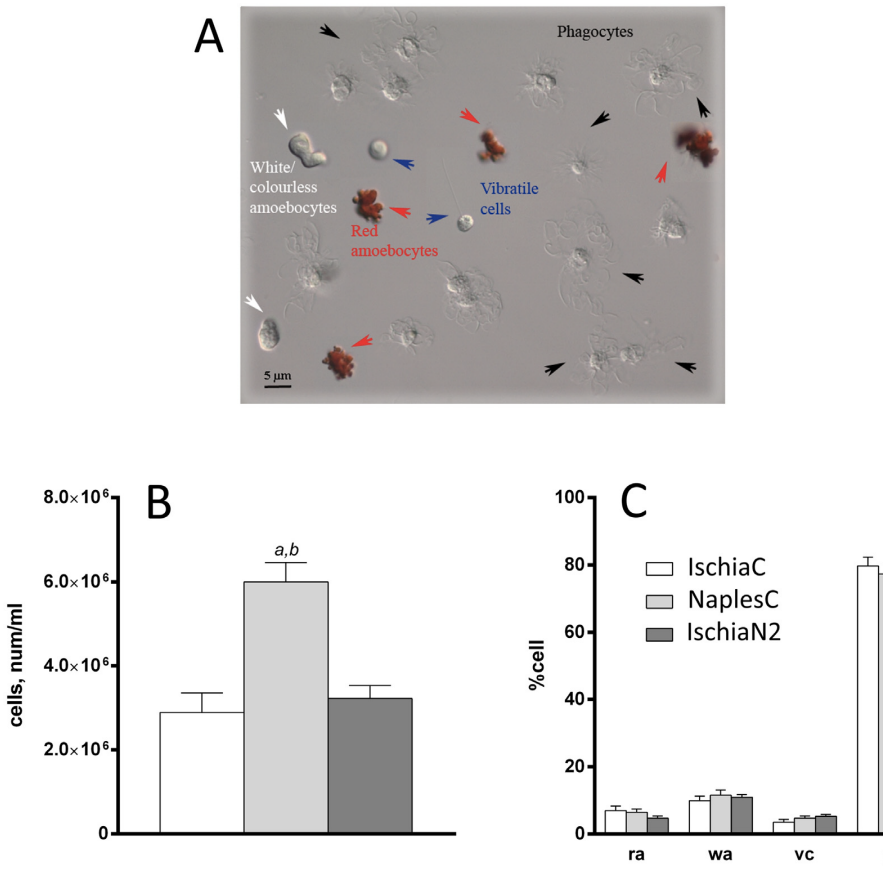

Fig. 1. Immune cells in Paracentrotus lividus. (A) Phagocytes (black arrows); red amoebocytes (red arrows);white/colourless amoebocytes (white arrows) and vibratile cells (blue arrows). (B) Total immune cells count; a, significant difference between IschiaC and NaplesC (P b 0.0001); b, significant difference between NaplesC and IschiaN2 (P b 0.0001) (see Table S1). (C) Percent distribution of cell types in sea urchins collected at IschiaN2 and control sites IschiaC and NaplesC (see Table S2). Bars represent mean ± SE (n = 10). ra = red amoebocytes, wa = white amoebocytes, vc = vibratile cells, p = phagocytes. (For interpretation of the references to colour in this figure legend, the reader is referred to the web version of this article.)

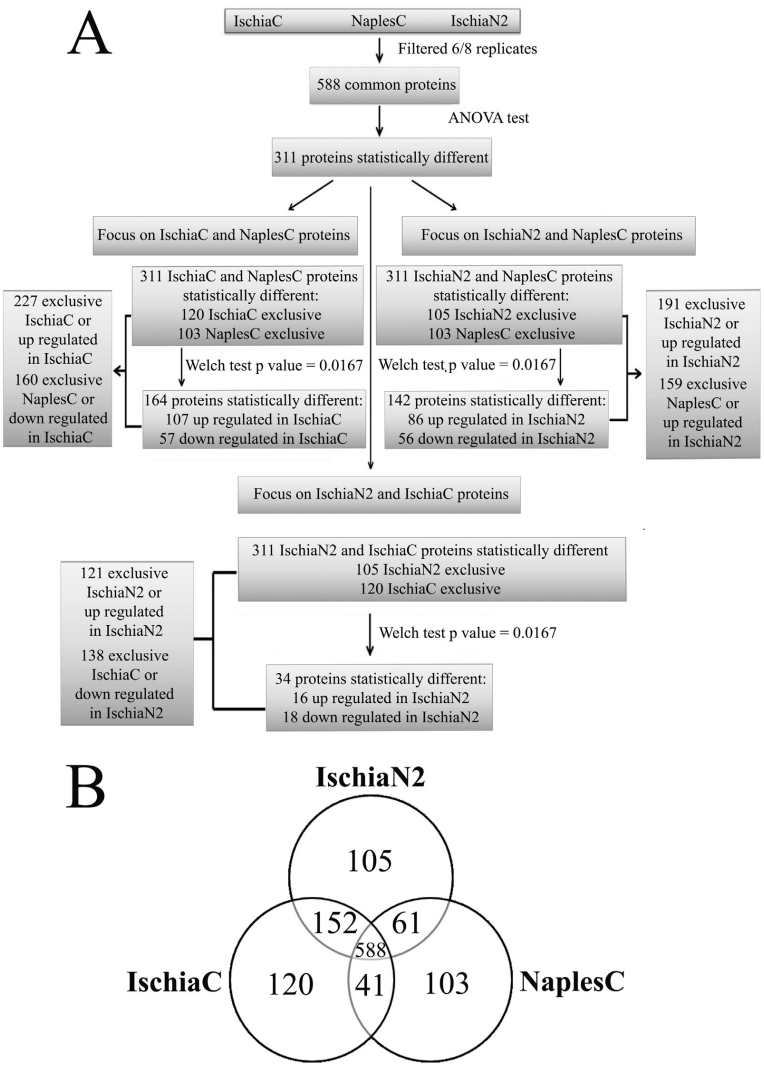

Fig. 2. Proteomic workflow and Venn diagram comparing the proteome of the immune cells from IschiaN2, IschiaC and NaplesC sea urchins. (A) Shotgun proteomic analysis was performed on sea urchins proteome from IschiaC, NaplesC and IschiaN2 sites. Statistical analyses were performed using the Perseus software (version 1.4.0.6, www.biochem.mpg.de/ mann/tools/). (B) Venn diagram showing the individual and shared proteins in sea urchins across sites. Only proteins present and quantified in at least 6 out of 8 repeats were considered as positively identified in a sample and used for statistical analyses.

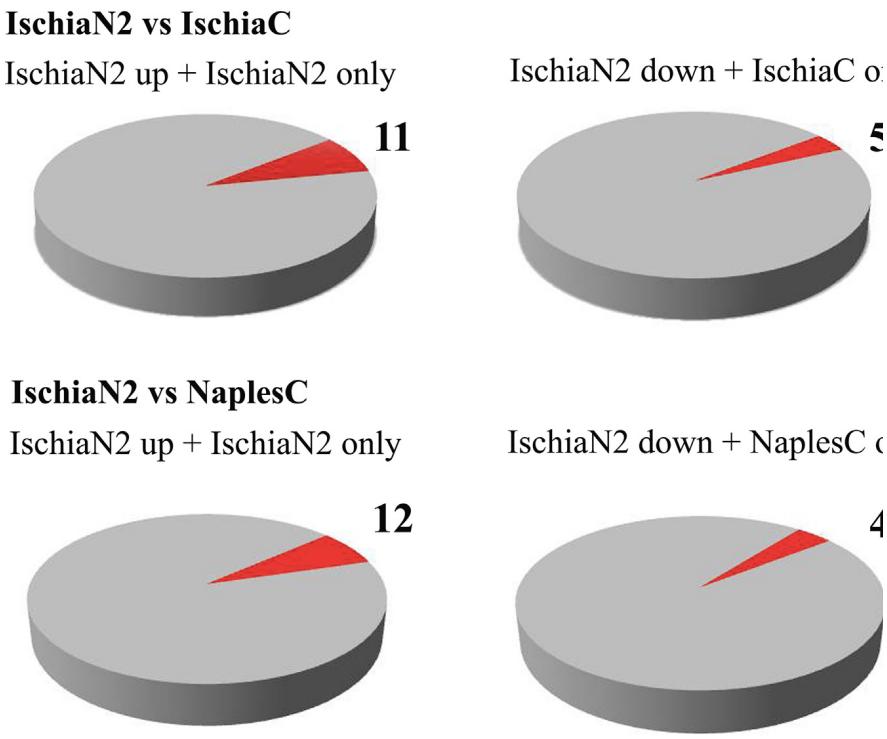

Fig. 3. Pie charts of the number of enzymes involved in oxidative processes, which are differentially expressed in immune cells from IschiaN2, IschiaC and NaplesC sea urchins. Numbers next to the red sections refer to the protein category count. (For interpretation of the references to colour in this figure legend, the reader is referred to the web version of this article.)

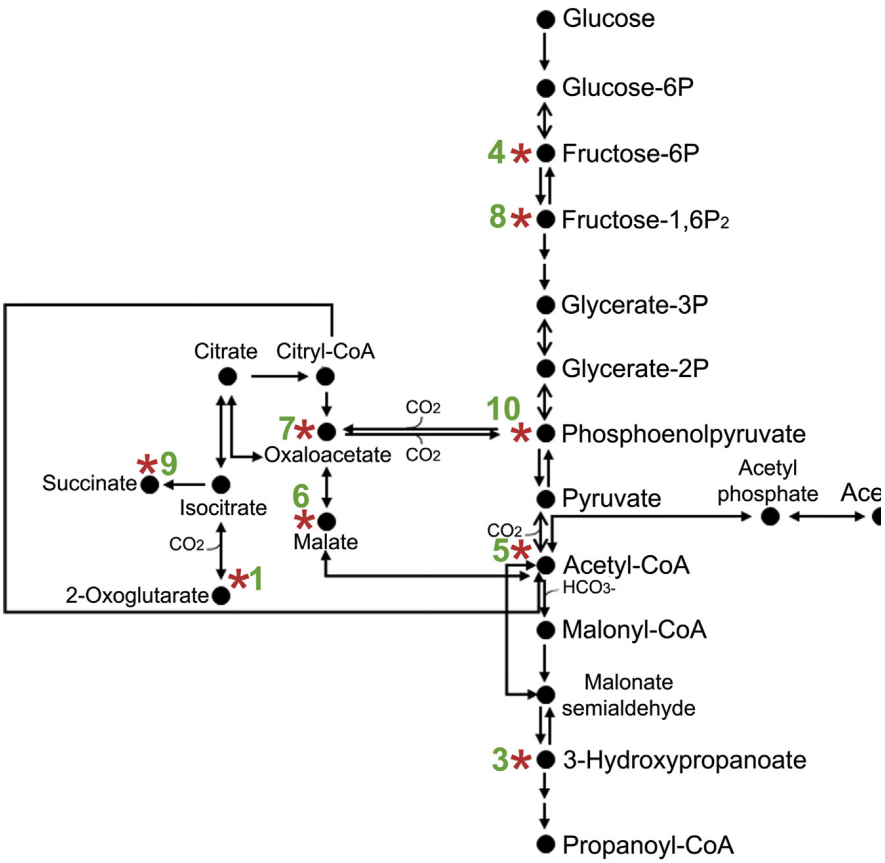

Fig. 4. Carbon metabolic pathways. The enzymes up or down-regulated in immune cells in a comparison IschiaN2 versus IschiaC are indicated by stars. 1, glutamate dehydrogenase mitochondrial; 2, acetyl-coenzyme A synthetase; 3, enoyl CoA hydratase; 4, glucose-6-phosphate isomerase; 5, acetyl-coenzyme A synthetase 2; 6, malate dehydrogenase; 7, aspartate aminotransferase; 8, fructose-1,6-bisphosphatase 1; 9, succinyl-CoA ligase subunit alpha; 10, pyruvate kinase.

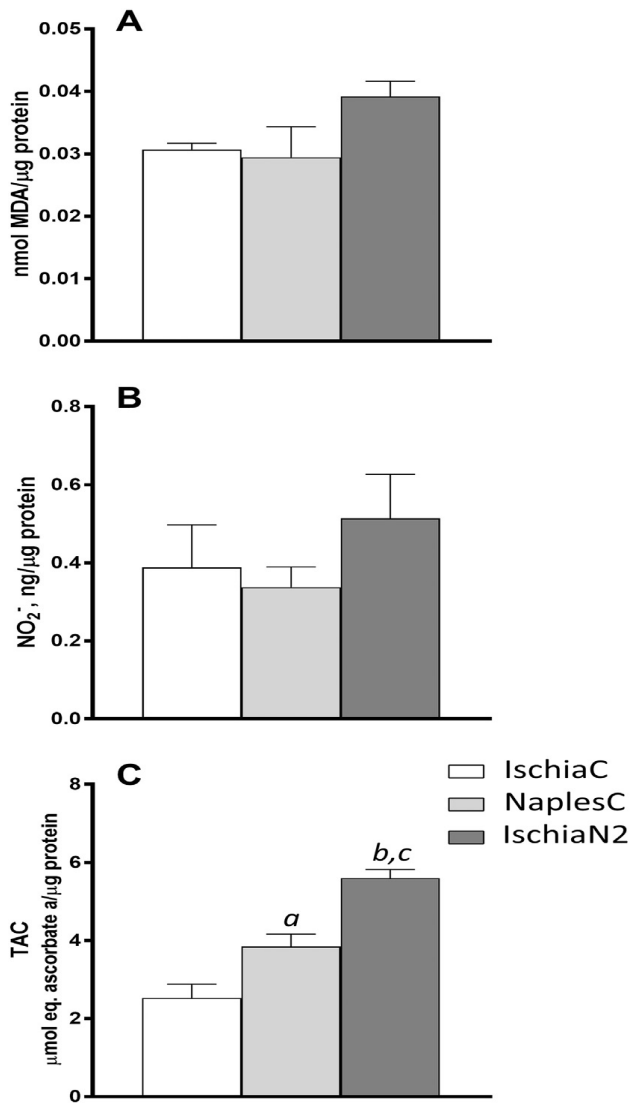

Fig. 5. Intracellular redox state in immune cells of urchins from the three sites. (A) Lipid peroxidation, (B) Nitric oxide production and (C) TAC; a, significant difference between IschiaC and NaplesC (P b 0.01); b, significant difference between NaplesC and IschiaN2 (P b 0.05); c, significant difference between IschiaC and IschiaN2 (P b 0.0001) (see Table S1). Bars represent mean ± SE (n = 6 in A, B and C).

IschiaN2 *vs* IschiaC: proteins up-regulated or only expressed in IschiaN2

Category	Term	Count	*P* Value	Genes
KEGG_PATHWAY	**spu00010:Glycolysis/Gluconeogenesis**	**4**	**0.00732**	**LOC593236, LOC592086, LOC762939, LOC585742**
KEGG_PATHWAY	spu01200:Carbon metabolism	5	0.00827	LOC584300, LOC592086, ECHS1, LOC762939, LOC585742
KEGG_PATHWAY	spu03040:Spliceosome	5	0.01552	LOC587779, LOC580001, LOC581143, LOC588126, LOC583936
KEGG_PATHWAY	**spu00640:Propanoate metabolism**	**3**	**0.01647**	**LOC592086, ECHS1, LOC585742**
KEGG_PATHWAY	**spu04145:Phagosome**	**4**	**0.02511**	**LOC574968, C3, LOC752782, LOC592912**
KEGG_PATHWAY	**spu00620:Pyruvate metabolism**	**3**	**0.03637**	**LOC593236, LOC592086, LOC585742**
INTERPRO	IPR020946:Flavin monooxygenase-like	2	0.04398	LOC579836, LOC586240
INTERPRO	**IPR012143:Dimethylaniline monooxygenase, N-oxid)-forming**	**2**	**0.04398**	**LOC579836, LOC586240**
INTERPRO	IPR000960:Flavin monooxygenase FMO	2	0.04398	LOC579836, LOC586240
UP_KEYWORDS	**Microsome**	**2**	**0.04787**	**LOC579836, LOC586240**
INTERPRO	IPR014014:RNA helicase, DEAD-box type, Q motif	2	0.05254	LOC580001, VASA

IschiaN2 *vs* NaplesC: proteins up-regulated or only expressed in IschiaN2

Category	Term	Count	*P* Value	Genes
UP_KEYWORDS	Nucleotide-binding	9	0.0046	LOC574813, GNAQ, LOC373525, LOC752782, LOC592912, LOC581673, VASA, LOC37
KEGG_PATHWAY	spu03010:Ribosome	8	0.00655	LOC580148, LOC752626, RPS14, LOC580462, LOC576368, LOC764368, LOC586110, L
KEGG_PATHWAY	spu00640:Propanoate metabolism	4	0.0097	LOC592086, LOC581673, ECHS1, LOC585742
KEGG_PATHWAY	spu01200:Carbon metabolism	6	0.03727	LOC588688, LOC575941, LOC592086, LOC581673, ECHS1, LOC585742
UP_KEYWORDS	ATP-binding	6	0.03821	LOC373525, LOC752782, LOC592912, VASA, LOC373382, SPIO
KEGG_PATHWAY	**spu04145:Phagosome**	**5**	**0.05614**	**LOC373365, LOC574968, LOC752782, LOC592912, LOC590813**

IschiaN2 *vs* IschiaC: proteins down regulated in IschiaN2 or only expressed in IschiaC

Category	Term	Count	*P* Value	Genes
INTERPRO	IPR027417:P-loop containing nucleoside triphosphate hydrolase	7	0.00593	LOC585853, LOC593133, LOC575255, LOC578813, LOC373178, LOC585398, LOC581
KEGG_PATHWAY	spu04144:Endocytosis	7	0.00646	LOC765161, LOC752803, LOC578960, LOC575255, LOC579715, LOC373178, LOC585
INTERPRO	IPR005225:Small GTP-binding protein domain	4	0.00725	LOC585853, LOC575255, LOC585398, LOC581537
SMART	SM00175:SM00175	3	0.01099	LOC575255, LOC585398, LOC581537
INTERPRO	IPR003579:Small GTPase superfamily, Rab type	3	0.01289	LOC575255, LOC585398, LOC581537
SMART	SM00176:SM00176	2	0.02147	LOC585398, LOC581537
INTERPRO	IPR002041:Ran GTPase	2	0.02273	LOC585398, LOC581537
KEGG_PATHWAY	spu01200:Carbon metabolism	5	0.0236	LOC577019, LOC592180, LOC577064, LOC581456, LOC592628
INTERPRO	IPR001806:Small GTPase superfamily	3	0.04013	LOC575255, LOC585398, LOC581537
SMART	SM00174:SM00174	2	0.04944	LOC585398, LOC581537
INTERPRO	IPR001878:Small GTPase superfamily, Rho type	2	0.05227	LOC585398, LOC581537
SMART	SM00173:SM00173	2	0.05632	LOC585398, LOC581537

IschiaN2 *vs* NaplesC: proteins down-regulated in IschiaN2 or only expressed in NaplesC

Category	Term	Count	*P* Value	Genes
SMART	SM00054:SM00054	3	0.01724	576,455, 578,403, 586,242
KEGG_PATHWAY	spu03050:Proteasome	4	0.02455	590,127, 754,955, 576,830, 591,581
INTERPRO	IPR018247:EF-Hand 1, calcium-binding site	3	0.0302	576,455, 578,403, 586,242
KEGG_PATHWAY	spu03010:Ribosome	6	0.03705	584,812, 593,861, 577,989, 578,034, 577,738, 579,026
INTERPRO	IPR002048:EF-hand domain	3	0.04368	576,455, 578,403, 586,242
INTERPRO	IPR011992:EF-hand-like domain	3	0.055	576,455, 578,403, 586,242

Table 1

Bioinformatic analysis of proteins differentially expressed. The analysiswas carried out by DAVID on the proteins differentially expressed in the comparison IschiaN2 versus IschiaC and IschiaN2 versus NaplesC. Only enriched categories with a P value ≤0.05 are reported.